

# Finite Element Analysis of Thermoelastic Instability of Disc Brakes

S. P. Jung, T. W. Park, J. H. Lee, W. H. Kim, and W. S. Chung

**Abstract**—In this study, the thermoelastic instability (TEI) was analyzed using the finite element analysis technique. The governing dynamic and heat equations were described. Three dimensional thermomechanical analysis model of the disc brake system were created. An intermediate processor based on the staggered approach was used to exchange result data: temperature, friction contact power, nodal displacement and deformation. Disc thickness variation (DTV) and temperature distribution of the disc were calculated, and the tendency and meaning of each result were discussed.

**Index Terms**—Thermoelastic instability, Finite element analysis technique, Thermomechanical analysis, Intermediate processor, Disc thickness variation

## I. INTRODUCTION

The friction heat generated between two sliding bodies causes thermoelastic deformation which alters the contact pressure distribution. This coupled thermo-mechanical process is referred to as frictionally-excited thermoelastic instability or TEI [1]. If the sliding speed is above one called critical speed, the resulting thermo-mechanical feedback is unstable, leading to the development of non-uniform contact pressure and local high temperature with important gradients called ‘hot spots’ [2]. The formation of such localized hot spots is accompanied by high local stresses that can lead to material degradation and eventual failure [3]. Also, the hot spots can be a source of undesirable frictional vibrations, known in the automotive disc brake community as ‘hot roughness’ or ‘hot judder’ [4].

In this study, a transient FE analysis method was used to analyze the fully coupled thermoelastic instability problem for a disc brake system. Mechanical and thermal model for the disc brake were generated separately, and solved iteratively using the staggered approach [5]. The staggered approach is one of the most popular computation techniques used to solve the highly coupled non-linear equations. Three dimensional FE model of a disc brake was created. The mechanical model of the disc brake was assumed to be in braking with an acceleration of 0.3g from 160 kph to 80kph. The thermal model with an initial temperature of 80°C

interacts with the mechanical model, and the friction heat between the pad and disc is generated by the contact condition. Due to the heat generation, the material of disc is expanded and alters the contact condition. By comparing the simulation results to the test data in Part.2 of this paper, the reliability of the FE models and computation scheme is verified.

## II. THEORETICAL BACKGROUND

The equation of motion of a constrained dynamic system is introduced based on the finite element approach [6]. The general heat equation is briefly reviewed and the basic strategy to analyze the coupled thermo-mechanical system is described according to the staggered approach.

### A. Dynamics of a Constrained Flexible Multibody System

The constraints on the system are efficiently taken into account using the Augmented Lagrangian method. The augmented functional of Hamilton’s principle is

$$\int_{t_1}^{t_2} \left[ \delta(L - k\lambda^T \Phi - \frac{p}{2} \Phi^T \Phi) + \delta W \right] dt = 0 \quad (1)$$

where  $k$  is the scaling factor and  $p$  is the penalty coefficient.  $\lambda$  is the vector of Lagrange multipliers and  $\Phi$  is the vector of constraints.  $L$  is the Lagrangian of the mechanism defined as  $L = T - V$ .  $T$  and  $V$  are the kinetic and potential energies of the system, respectively.  $W$  is the virtual work of external forces. Using the virtual displacement principle, the motion equations are obtained as

$$\begin{cases} \frac{d}{dt} \left( \frac{\partial L}{\partial \dot{q}} \right) - \frac{\partial L}{\partial q} = Q - (k\lambda + p\Phi) \frac{\partial \Phi}{\partial q} \\ k\Phi(q, t) = 0 \end{cases} \quad (2)$$

where  $q$  is the vector of generalized coordinates. Equation (2) can be written in the matrix form

$$\begin{cases} M\ddot{q} + B^T(p\Phi + k\lambda) = g(q, \dot{q}, t) \\ k\Phi(q, t) = 0 \end{cases} \quad (3)$$

where  $B$  is the gradient matrix of the constraints

Manuscript received March 5, 2010. This work was supported by Korea Institute for Advancement of Technology.

S. P. Jung is a PhD candidate student. (e-mail: moonsejung@naver.com)

T. W. Park is a professor of Ajou University, Suwon, Republic of Korea. (Phone: +82-31-219-2952; fax: +82-31-219-1965; e-mail: park@ajou.ac.kr)

J. H. Lee and W. H. Kim are in the course of master’s degree. (e-mail: ljh1227@ajou.ac.kr, shornet@nate.com)

W. S. Chung is a senior researcher of Korea Automotive Technology Institute. (e-mail: wschung@katech.re.kr)

$(B = \frac{\partial \Phi}{\partial q})$  and  $g$  is the vector of apparent force

$$g = Q - \frac{\partial L}{\partial q} - \frac{\partial}{\partial q} \left( \frac{\partial L}{\partial \dot{q}} \dot{q} \right) \quad (4)$$

The linearized form of the motion (65) can be described as

$$\begin{bmatrix} M & 0 \\ 0 & 0 \end{bmatrix} \begin{bmatrix} \Delta \ddot{q} \\ \Delta \ddot{\lambda} \end{bmatrix} + \begin{bmatrix} C_T & 0 \\ 0 & 0 \end{bmatrix} \begin{bmatrix} \Delta \dot{q} \\ \Delta \dot{\lambda} \end{bmatrix} + \begin{bmatrix} K_T & kB^T \\ kB & 0 \end{bmatrix} \begin{bmatrix} \Delta q \\ \Delta \lambda \end{bmatrix} = \begin{bmatrix} r^* \\ -\Phi^* \end{bmatrix} \quad (5)$$

### B. Transient Computation of Heat Transfer Equation

The temperature within in an element is computed based on the nodal temperature vector

$$T(x, t) = \phi(x) \cdot T(t) \quad (7)$$

where  $x$  is the nodal coordinate,  $\phi(x)$  is the interpolation function vector and  $T(t)$  is the nodal temperature vector. The governing equation of the heat transfer problem is

$$C(T)\dot{T} + K(T)T = Q(T) \quad (8)$$

where  $C(T)$  and  $K(T)$  are the discretised system's temperature-dependant heat capacity and thermal conductivity matrices, respectively,  $T$  is the nodal temperature vector,  $\dot{T}$  is the time derivative of the temperature vector, and  $Q(T)$  is the heat flux vector. The solution vector  $T_\gamma$  of Equation (11) at time  $\gamma$ , which is located at time intervals between  $n$  and  $n+1$  step, can be expressed as

$$T_\gamma = (1 - \gamma)T_n + \gamma T_{n+1} \quad (9)$$

The variation rate of the temperature can be written as

$$\dot{T}_\gamma = \frac{1}{\gamma \Delta t} (T_r - T_n) \quad (10)$$

### C. Heat Generation Due to Friction Contact

In disc brakes, the friction heat is generated between the disc and pads. Frictional heat generation per unit time at the node  $i$  is calculated as

$$q_{cf}^i = \eta \mu \sigma_c \nu \quad (11)$$

where  $\eta$  is the factor defining the percentage of

mechanical power converted into heat,  $\mu$  is the friction coefficient,  $\sigma_c$  is the contact pressure and  $\nu$  is the local velocity. The amount of heat going to the contractor and target bodies,  $q_1^i$  and  $q_2^i$ , are determined with the parameter  $\varpi$

$$q_1^i = \frac{\varpi}{1 + \varpi} q_{cf}^i, \quad q_2^i = \frac{1}{1 + \varpi} q_{cf}^i \quad (12)$$

### D. Computation Strategy

Figure 1 shows the computational analysis strategy used in this study. The thermal model can send the nodal temperature to the mechanical model. The mechanical model transfers the nodal position, power and contact pressure to the thermal model. At time  $(t) = 0$ , the initial static computation results of the mechanical model and the initial steady-state computation results of the thermal model are exchanged. In step 1, the nodal temperature distribution is updated considering the initial deformation and power of the mechanical model. In step 2, using the nodal temperature, the deformation of material is calculated. This affects on constraints including the contact condition, and if the deformation of the material due to the temperature is too large, the Newton-Raphson iteration can be failed to converge. The power due to plastic deformation and friction contact is computed in this step. In step 3, the power is transferred to the heat and the heat is applied to the thermal model as a thermal load. At this step, the temperature distribution of nodal point is estimated in equilibrium state. Step 2 and 3 are repeated until the calculation time ends. At every step, the time step is controlled automatically according to the residue of equation (9) and (11) and if the residue doesn't converge in the allowed number of iterations, calculation stops.

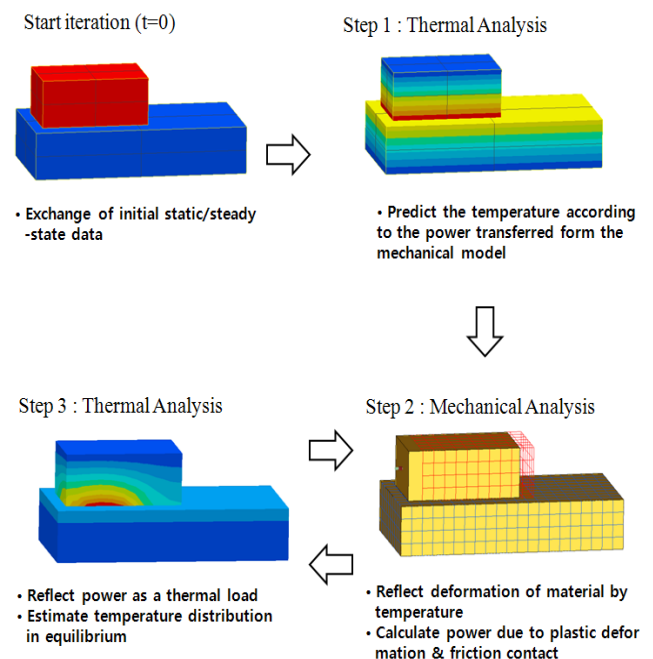


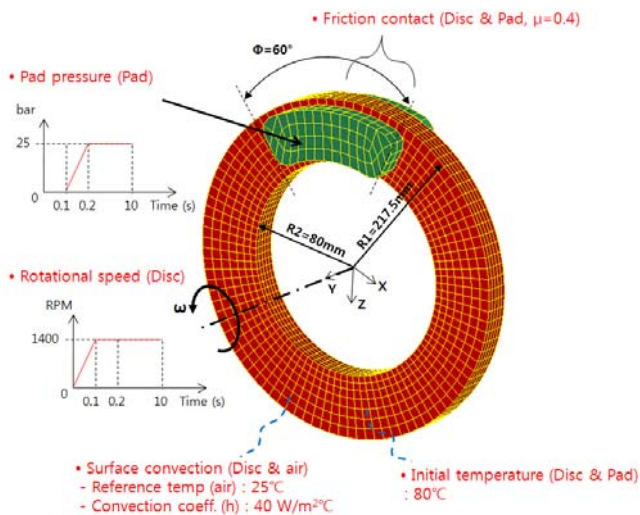
Figure 1. Analysis strategy based on the staggered

approach

### III. SIMULATION

#### A. Finite Element Model

Figure 2 shows the finite element model and boundary conditions of the simple disc brake module composed of a disc and two pads. The outer radius ( $R_1$ ) and inner radius ( $R_2$ ) of the disc are 127.5 mm and 80 mm. The effective angle of the pad ( $\Phi$ ) is  $60^\circ$  and the thickness of the disc and pad is 19 mm and 15 mm, respectively. The disc is constrained on the ground with a hinge joint and rotates with a constant rotational speed ( $\omega$ ) of 1400 rpm. The pad can move in z-direction and a constant pressure of 25 bar pushes on the surface of the pad. The friction contact conditions are applied between the surfaces of the disc and pads with the friction coefficient ( $\mu$ ) of 0.4. To avoid a singularity problem and reduce a computational effort, the rotational speed of the disc increases from 0 rpm to 1400 rpm for 0.1 second. When the rotational speed of the disc reaches its maximum, the pad starts to move. So, it is not necessary to perform the static analysis of the dynamic model at  $t = 0$  second and the friction contact condition converges in a small number of the Newton-Raphson iterations since the pad contacts on the disc when dynamic status of the disc is stable. The boundary conditions of the thermal model are also described in Figure 2, and it is quite simple. The initial temperature of the disc and pads is  $80^\circ\text{C}$ , and the surface convection condition is applied at all surfaces of the disc with the reference temperature (air) of  $25^\circ\text{C}$  and the convection coefficient ( $h$ ) of  $40 \text{ W/m}^2\text{C}$ . 8-nodes hexahedron elements are used and all parts are assumed to be aluminum.



#### B. Simulation Results

Figure 4 shows the change of the temperature distribution of the disc surface in radial direction according to time. The temperature of the disc is  $80^\circ\text{C}$  at  $t = 0\text{s}$  and increases to its maximum of  $442^\circ\text{C}$  at  $t = 10\text{s}$ . It is shown that the temperature of the inner region of the disc is higher than that of the outer region. The hinge joint was set between the

ground and the nodes of the surface of the disc inner circle (refer to Figure 5), and rotates the nodes compulsorily by 1400 rpm. Thus, the reaction stress is concentrated at the nodes located at the surface of the disc inner circle and the contact pressure and temperature are increased.

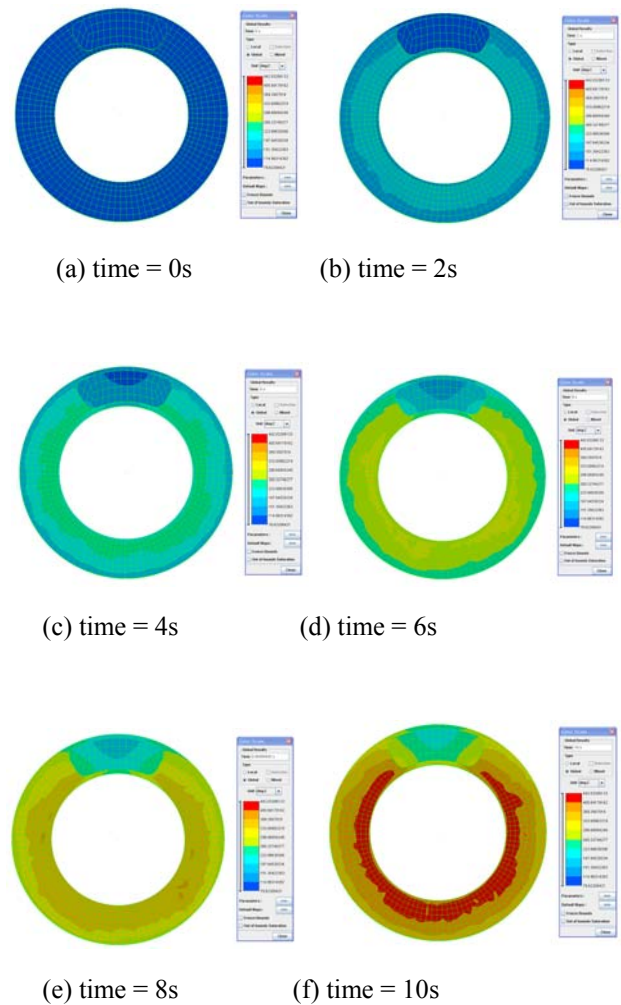


Figure 4. Change of the temperature distribution of the disc surface in radial direction according to time

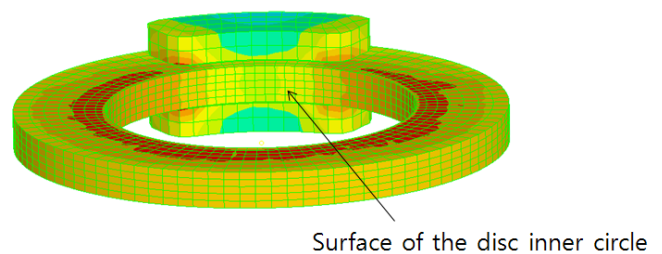
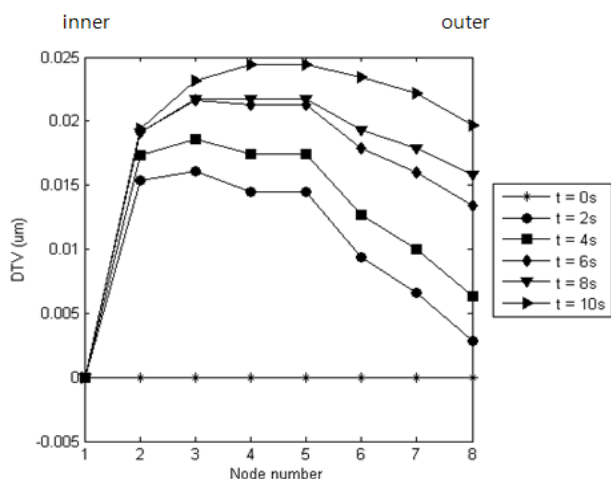


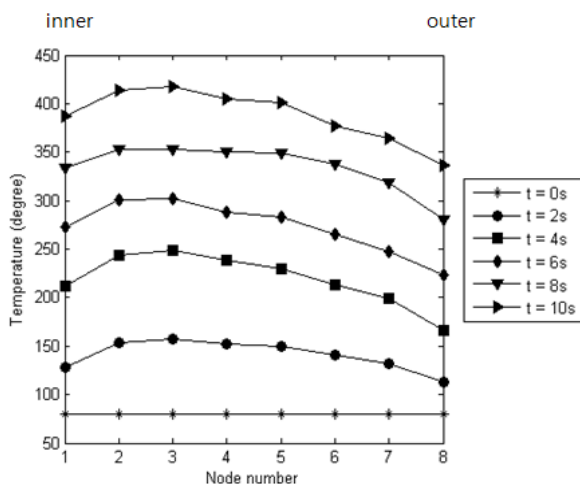
Figure 5. Temperature variation of the disc and pads in axial direction

Figure 6 (a), (b) shows the disc thickness variation (DTV) and temperature variation of the disc surface along the radial direction of the disc. In Figure 6 (a), DTV of node 1, which is located at the surface of the disc inner circle, is almost zero. Because 6-DOF of node 1 is fixed with the disc center node where the hinge joint is equipped, translation in y-axes, which is the same direction with the rotational axes of the

disc, is constrained, and then the resultant DTV is zero. DTV is sharply increased at node 2 since the contact pressure and temperature are concentrated at this region. DTV keeps an almost constant level between nodes 2 and 5, then decreases. As time increasing, DTV is also increasing because of the contact pressure improvement by the thermal expansion of materials of the disc and pads. The magnitude of the thermal expansion becomes bigger as temperature rise. Figure 6 (b) shows the temperature at each node is increasing according to time, and the maximum temperature can be measured at node 2 and 3.



(a) Disc thickness variation (DTV)



(b) Temperature variation of the disc surface

Figure 6. Disc thickness and temperature variation along the radial direction of the disc

#### IV. CONCLUSION

Thermoelastic instability (TEI) of the disc brake system is discussed in this paper. A simple finite element model of a disc and two pads was created, and TEI phenomenon was implemented by rotating the disc with a constant rotational speed of 1400 rpm. The intermediate processor using the

staggered approach was used to connect results of two other analysis domains: mechanical and thermal analysis. By exchanging calculation results such as temperature distribution, contact power and nodal position at every time step, solutions of fully coupled thermo-mechanical system could be obtained. Contact pressure distribution of the pad surface was varied according to the rotational direction of the disc. DTV and temperature of the disc were calculated and tendency was verified by earlier studies. In the near future, the analysis technique is going to be applied to the actual disc brake module and the result will be compare with the experiment.

#### REFERENCES

- [1] K. J. Lee and J. R. Barber, "An Experimental Investigation of Frictionally-Excited Thermoelastic Instability in Automotive Disk Brakes Under a Drag Brake Application", *Journal of Tribology*, vol. 116, 1994, pp. 409-414.
- [2] O. Altuzarra, E. Amezcua, R. Aviles and A. Hernandez, "Judder vibration in disc brakes excited by thermoelastic instability", *Engineering computations*, vol. 19, no. 4, 2002, pp. 411-430.
- [3] Y. H. Jang and S. H. Ahn, "Frictionally-excited thermoelastic instability in functionally graded material", *Wear*, vol.262, 2007, pp.1102-1112.
- [4] B. Y. Yi, J. R. Barber and P. Zagrodzki, "Eigenvalue solution of thermoelastic instability problems using Fourier reduction", *Proceedings of the Royal Society of London A*, vol.456, 2000, pp. 2799-282.
- [5] G. H. Yoon and O. Sigmund, "A monolithic approach for topology optimization of electrostatically actuated devices", *Computer Methods in Applied Mechanics and Engineering*, vol. 197, 2008, pp. 4062-4075.
- [6] M. Geradin and A. Cardona, *Flexible Multibody Dynamics*, John Willey & Sons, Chichester, England, 2000.